Electric Power Systems Research 213 (2022) 108784

Contents lists available at ScienceDirect

Electric Power Systems Research

journal homepage: www.elsevier.com/locate/epsr

Comparison of far electric field waveforms produced by rocket-triggered lightning strokes and subsequent strokes in natural lightning

Z. Ding [a,*], S. Chen [a], V.A. Rakov [a], Y. Zhu [b], I. Kereszy [a], M.A. Uman [a]

[a] Department of Electrical and Computer Engineering, University of Florida, Gainesville, FL, USA
[b] Earth Networks, Germantown, MD, USA

ARTICLE INFO

Keywords:
Rocket-and-wire triggered lightning
Natural lightning
Subsequent return stroke
Electric field waveform
10-to-90% risetime
Half-peak width
Initial half-cycle duration
Oppostie polarity overshoot
Slow front

ABSTRACT

Using wideband electric field records obtained at the Lightning Observatory in Gainesville (LOG), Florida, we examined in detail the characteristics of far electric field waveforms produced by two categories of lightning return strokes. The first category includes return strokes of any order in lightning flashes triggered by a rocket extending a grounded wire toward the overhead thundercloud, which we label RTL (rocket-triggered lightning) strokes. The second category includes return strokes of order 2 and higher (that is, only subsequent strokes) in natural cloud-to-ground lightning flashes, which we label NL (natural lightning) strokes. Properties of RTL and NL strokes are expected to be similar. A total of 139 RTL strokes from years 2013 to 2016 and 184 NL strokes from years 2013 to 2015 were examined in this study. All strokes transported negative charge to ground and occurred at similar distances from LOG. Similarities and dissimilarities of waveform parameters for the two categories of strokes and their possible explanations are discussed in this paper. This is the first detailed comparison of electric field waveforms of RTL and NL strokes recorded at approximately the same distance (some tens of kilometers) and with the same instrumentation.

1. Introduction

It is commonly assumed (e.g., Rakov & Uman, 2003 [1]) that rocket-and-wire triggered lightning strokes are similar or even identical to subsequent (as opposed to first) strokes in natural lightning. This assumption is largely based on works of Le Vine et al. [1989] [2] and Fisher et al. [1993] [3].

The initial rising part of return-stroke electric field waveform is traditionally characterized as composed of a 'slow front' and a 'fast transition'. Weidman & Krider [1978] [4] have reported characteristics of slow front for both first and subsequent return strokes in natural lightning. They measured electric fields at distances of 50–200 km, with field propagation being over seawater. Nag et al. [2012] [5] studied the fine structure of electric field waveforms recorded at near (0.5 - 3.6 km) and far (around 50 km) distances for first strokes in natural lightning, with propagation path being over land. Mallick and Rakov [2014] [6] examined electric field waveforms produced by 69 negative return strokes in 13 flashes triggered using the rocket-and-wire technique at Camp Blanding (CB), Florida, in 2012. The field waveforms were recorded at the Lightning Observatory in Gainesville (LOG), at a distance of 45 km from the lightning channel. They compared their rocket-and-wire triggered lightning data with natural lightning data found in the literature.

In this paper, we will label the return strokes of any order in rocket-and-wire triggered lightning "RTL strokes", and return strokes of order 2 and higher (that is, only subsequent strokes) in natural lightning will be labeled "NL strokes". No first strokes in natural lightning were considered, because there is nothing to compare them to in rocket-and-wire triggered lightning, in which the first stroke is in effect replaced with the so-called initial-stage processes (e.g. Rakov and Uman, 2003, Chapter 7 [1]). Note that properties of first strokes in NL differ significantly from those of subsequent strokes, because the first-stroke leader has to move through virgin air and is associated with a larger electric charge. Subsequent-stroke leaders usually retrace the remnants of the preceding-stroke channel and transfer smaller electric charges than their first-stroke counterparts. As described in Section 3, we have identified subsequent strokes in NL that likely created a new termination on ground (that is, did not fully remain in the previously conditioned channel to ground) and removed them from our dataset. All strokes examined in this study transported negative charge to ground. All RTL

* Corresponding author at: Electrical and Computer Engineering, University of Florida, 1604 Center Dr, New Engineering Building Room 556, Gainesville, Florida, 32611, USA.
E-mail address: ziqinding94@ufl.edu (Z. Ding).

https://doi.org/10.1016/j.epsr.2022.108784
Received 20 June 2022; Received in revised form 16 August 2022; Accepted 30 August 2022
Available online 8 September 2022

strokes occurred in flashes initiated using the classical (grounded-wire) triggering technique at the Camp Blanding (CB) lightning triggering facility, at a distance of 45 km from LOG.

This work can be viewed as an extension of that of Mallick and Rakov (2014) [6]. We have used a larger sample of RTL events and included new data for NL events occurring at distances similar to that of the RTL events, with both the RTL and NL events being recorded with the same instrumentation installed at LOG. Specifically, we examined 139 RTL strokes from 26 flashes triggered from 2013 to 2016 vs. 69 RTL strokes from 13 flashes triggered in 2012 in Mallick and Rakov's study. Further, electric field waveforms of 184 NL strokes from 46 flashes at distances of 35 to 55 km from LOG, similar to the 45 km distance for RTL strokes, recorded in years 2013 and 2015, were included in our analysis. Both RTL and NL data were acquired in the summertime.

The total electric field produced by a lightning return stroke consists of the electrostatic, induction, and radiation components, with contributions of the individual components varying with distance (e.g., Rakov and Uman, 2003, Chapter 4 [1]). This paper focuses on electric field waveforms produced by both RTL and NL strokes at relatively far distances, where the electric field waveform (particularly its initial part, 10 μs or so) is dominated by its radiation component. For all RTL strokes, the distance is fixed at 45 km (the distance between CB and LOG). NL strokes used in this study were selected from our database so that their locations reported by the National Lightning Detection Network (NLDN) are not far from CB, as illustrated in Fig. 1. Thus, for all the examined strokes, the influence of distance (propagation path) on field waveforms, including attenuation and distortion due to finite ground conductivity, is approximately the same. The larger sample size for RTL strokes and the use of NL strokes from a more or less the same region, with all the data being recorded with the same instrumentation, make our RTL vs. NL comparison more meaningful than that previously performed by Mallick and Rakov [2014] [6]. For completeness, we have included Mallick and Rakov's results, as well as other results found in the literature (see Tables 1–8) in this paper, but the main focus here is on comparison of RTL and NL strokes which are recorded with the same instrumentation and for which any differences in the field propagation path are minimized.

2. Instrumentation

Electric field waveforms presented here were recorded at the Lightning Observatory in Gainesville (LOG), located 45 km from the Camp Blanding (CB) lightning triggering facility (see Fig. 1). The electric field measuring system at LOG had a bandwidth of 16 Hz to 10 MHz. The decay time constant was 10 ms. All waveforms were recorded with 12-bit vertical resolution and a sampling rate of 100 MHz (sampling interval of 10 ns).

For rocket-and-wire triggered lightning, LOG instrumentation was triggered via a dedicated phone line, which transmitted a trigger signal from CB to LOG in the event of a lightning discharge at CB (see Rakov et al. [2014] [7] for details). For natural lightning, LOG instrumentation was triggered by an oscilloscope at the Golf Course Station (GC), located about 3 km from CB, via the IP-addressed digital input and output (iPIO) devices and the internet. Relative positions of LOG, CB, and GC, three parts of the International Center for Lightning Research and Testing (ICLRT), are shown in Fig. 1. Locations of individual NL strokes (also shown in Fig. 1) were determined using NLDN data.

3. Methodology

As noted in Section 1, all strokes considered in this study (whether RTL or NL) were of subsequent type. Further, they all occurred within 35–55 km of LOG, and their wideband electric field signatures were recorded with the same instrumentation. In order to filter out

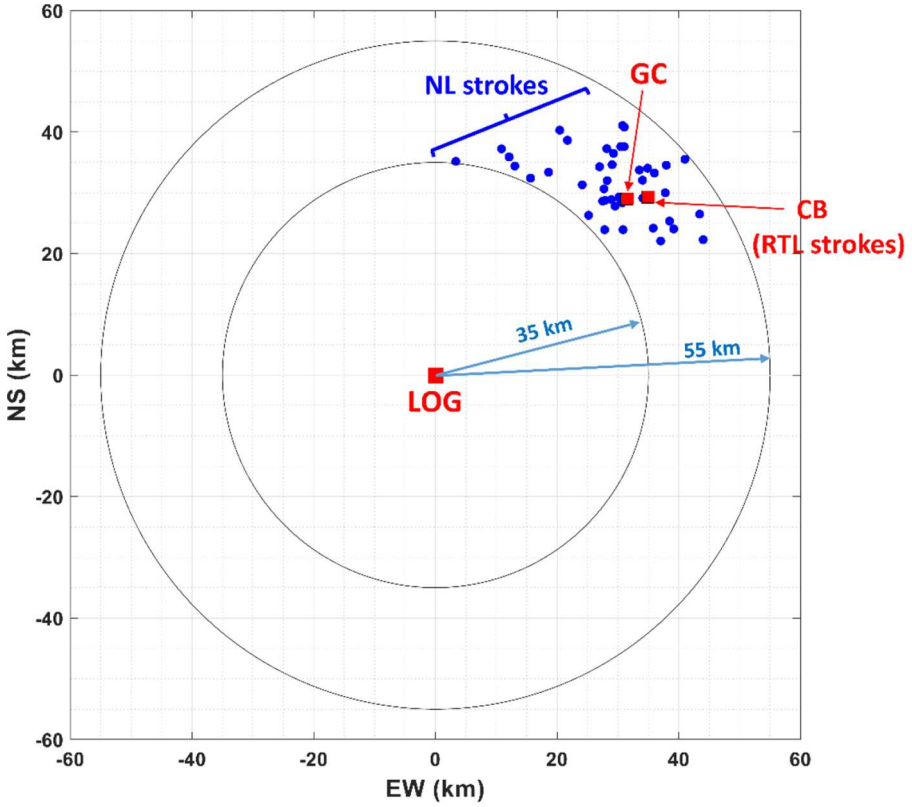

Fig. 1. Relative positions of Lightning Observatory in Gainesville (LOG); Camp Blanding lightning triggering facility (CB), and the Golf Course Station (GC). Blue circles represent the positions of 184 NL strokes in 46 flashes (positions of multiple strokes in the same flash are overlapped). The CB position represents the positions of all 139 RTL strokes examined in this study.

Table 1
10-to-90% risetime for RTL and NL strokes.

10-to-90% Risetime (μs)										
Reference	Location	Distance	N	AM	GM	Min	Max	SD	SE	SE,%
Master et al. (1984) [12] (NL)	Florida	1–20 km	220	1.5	–	–	–	0.9	0.06	4.0
Mallick and Rakov (2014) [6] [6] (RTL)	LOG	45 km	69	1.3	1.2	0.7	5.5	0.7	0.08	6.5
Wang et al. (2019) [30] (RTL)	Foshan	68–126 km	38	1.8	1.6	6	13.8	1.1	0.18	9.9
Present Study (RTL)	LOG	45 km	139	1.6*	1.5	1	7.7	0.82	0.07	4.3
Present Study (NL)	LOG	35–55 km	184	2.5*	2.2	0.91	7.5	1.2	0.09	3.6

* The difference in AM values for RTL and NL is statistically significant.

Table 2
Half-peak width for RTL and NL strokes.

Half-Peak Width (μs)										
Reference	Location	Distance	N	AM	GM	Min	Max	SD	SE	SE,%
Mallick and Rakov (2014) (RTL)	LOG	45 km	69	2.3	2.2	1.6	5.8	0.8	0.1	4.2
Wang et al. (2019) (RTL)	Foshan	68–126 km	38	2.9	2.9	1.1	14.8	1.2	0.19	6.7
Present Study (RTL)	LOG	45 km	139	3.8*	3.1	1.9	16	3	0.25	6.7
Present Study (NL)	LOG	35–55 km	184	6.3*	5.4	1.5	19	3.8	0.28	4.4

* The difference in AM values for RTL and NL is statistically significant.

Table 3
Initial half-cycle duration for RTL and NL strokes.

Initial Half-Cycle Duration or Zero-Crossing Time (μs)										
Reference	Location	Distance	N	AM	GM	Min	Max	SD	SE	SE,%
Lin et al. (1979) [13] (NL)	KSC	200 km	77	36	–	–	–	17	1.94	5.4
	Ocala	50 km	20	44	–	–	–	15	3.35	7.6
Cooray and Lundquist (1985) [14] (NL)	Sweden	–	94	39	–	–	–	8	0.83	2.1
	Sri Lanka	100–200 km	143	42	–	–	–	14	1.17	2.8
Haddad et al. (2012) [10] (NL)	LOG	10–50 km	152	58	55	–	–	–	–	–
		50–100 km	68	71	64	–	–	–	–	–
Mallick and Rakov (2014) (RTL)	LOG	45 km	15	50	48	28	71	12	3.1	6.2
Wang et al. (2019) (RTL)	Foshan	68–126 km	12	50	47	14	90	15	4.33	8.7
Present Study (RTL)	LOG	45 km	100	51*	45	6.8	127	21.1	2.1	4.2
Present Study (NL)	LOG	35–55 km	145	58*	53	9.1	132	23	1.91	3.3

* The difference in AM values for RTL and NL is not statistically significant.

Table 4
Opposite polarity overshoot duration for RTL and NL strokes.

Opposite Polarity Overshoot Duration (μs)										
Reference	Location	Distance	N	AM	GM	Min	Max	SD	SE	SE,%
Haddad et al. (2012) (NL)	LOG	10–50 km	152	20	15	–	–	–	–	–
		50–100 km	68	71	64	–	–	–	–	–
Mallick and Rakov (2014) (RTL)	LOG	45 km	15	44	40	20	77	18	4.65	10.6
Wang et al. (2019) (RTL)	Foshan	68–126 km	12	118	100	14	278	56	16.17	13.7
Present Study (RTL)	LOG	45 km	34	36.1*	27.2	3.2	93.6	24.7	4.23	11.7
Present Study (NL)	LOG	35–55 km	65	49.5*	38.5	8.4	182.4	36.6	4.54	9.2

* The difference in AM values for RTL and NL is not statistically significant.

Table 5
Ratio of electric field peak to opposite polarity overshoot for RTL and NL strokes.

Ratio of Electric Field Peak to Opposite Polarity Overshoot										
Reference	Location	Distance	N	AM	GM	Min	Max	SD	SE	SE,%
Haddad et al. (2012) (NL)	LOG	10–50 km	152	7.4	7.3	–	–	–	–	–
		50–100 km	68	64	39	–	–	–	–	–
Mallick and Rakov (2014) (RTL)	LOG	45 km	15	15.9	15.5	11	23.1	3.6	0.93	5.8
Wang et al. (2019) (RTL)	Foshan	68–126 km	12	7.2	6.7	2.7	25.6	3.8	1.1	15.2
Present Study (RTL)	LOG	45 km	34	23.3*	21	7.8	47.7	10.52	1.8	7.7
Present Study (NL)	LOG	35–55 km	65	13.8*	11.9	3.56	39.6	7.97	0.99	7.2

* The difference in AM values for RTL and NL is statistically significant.

subsequent strokes creating new terminations on ground, we did not include in our analysis any NL strokes that had leader durations (measured in our electric field records) longer than 8 ms. According to Rakov and Uman [2003, Chapter 4] [1], the geometric means of leader duration for subsequent strokes that follow the same channel and those creating new terminations on ground are well separated (1.5 to 2.6 ms

Table 6
Slow-front duration for RTL and NL strokes.

Slow-front duration (μs) Reference	Location	Distance	N	AM	GM	Min	Max	SD	SE	SE,%
Weidman and Krider (1978) [4] (NL)	Florida	50–200 km	44	0.6	–	–	–	0.2	0.03	5
			120	0.9	–	–	–	0.5	0.05	5.1
			34	2.1	–	–	–	0.9	0.15	7.3
Mallick and Rakov (2014) (RTL) (CT)	LOG	45 km	49	1.2	1.0	0.2	3.6	0.7	0.1	8.3
Mallick and Rakov (2014) (RTL) (PT)			7	22.8	–	–	–	–	–	–
Mallick and Rakov (2014) (RTL) (Combined)			56	3.9	2.1	0.23	15.5	–	–	–
Wang et al. (2019) (RTL)	Foshan	68–126 km	38	6.2	4.10	2	28.90	4.8	0.78	12.6
Present Study (RTL) (CT)	LOG	45 km	70	3.75*	2.12	0.3	19	4.44	0.53	14.2
Present Study (RTL) (PT)			58	8.19*	6.63	0.7	17.6	4.45	0.58	7.1
Present Study (RTL) (Combined)			128	5.81*	3.59	0.3	19	4.94	0.44	7.5
Present Study (NL) (CT)	LOG	35–55 km	112	3.91*	3.34	0.8	12	2.16	0.2	5.2
Present Study (NL) (PT)			41	7.42*	6.87	2.72	15.6	2.95	0.46	6.2
Present Study (NL) (Combined)			153	4.85*	4.06	0.8	15.6	2.85	0.23	4.8

* The difference in AM values for RTL and NL is not statistically significant.

Table 7
Slow-front magnitude relative to peak for RTL and NL strokes.

Slow-front magnitude relative to peak (%) Reference	Location	Distance	N	AM	GM	Min	Max	SD	SE	SE,%
Weidman and Krider (1978) (NL)	Florida	50–200 km	44	20	–	–	–	10	1.51	7.5
			120	25	–	–	–	10	0.91	3.7
			34	40	–	–	–	20	3.43	8.6
Mallick and Rakov (2014) (RTL) (CT)	LOG	45 km	49	9.9	9	3.3	19.8	4.5	0.64	6.5
Wang et al. (2019) (RTL)	Foshan	68–126 km	38	9.3	7.70	0.1	34.40	5.2	0.84	9.1
Present Study (RTL) (CT)	LOG	45 km	70	11.8*	10.7	2.5	26	5.15	0.62	5.2
Present Study (RTL) (PT)			58	10.1*	8.6	2.05	25.1	5.41	0.71	7.0
Present Study (RTL) (Combined)			128	11.1*	9.8	2.1	26	5.33	0.47	4.2
Present Study (NL) (CT)	LOG	35–55 km	112	12.0*	10.9	1.87	41.7	5.88	0.56	4.6
Present Study (NL) (PT)			41	12.0*	11.5	5.19	21.3	3.69	0.58	4.8
Present Study (NL) (Combined)			153	12.0*	11.0	1.87	41.7	5.37	0.43	3.6

* The difference in AM values for RTL and NL is not statistically significant.

Table 8
Fast-transition 10-to-90% risetime for RTL and NL strokes.

Fast-transition 10-to-90% risetime (μs) Reference	Location	Distance	N	AM	GM	Min	Max	SD	SE	SE,%
Weidman and Krider (1978) (NL)	Florida	50–200 km	80	0.2	–	–	–	0.04	0.004	2.2
			34	0.15	–	–	–	0.1	0.017	11.4
Master et al. (1984) (NL)	Florida	1–20 km	217	0.61	–	–	–	0.27	0.018	3.0
Mallick and Rakov (2014) (RTL)	LOG	45 km	69	0.99	0.98	0.74	1.56	0.13	0.016	1.6
Wang et al. (2019) (RTL)	Foshan	68–126 km	38	1.4	1.38	0.1	2.70	0.25	0.041	2.9
Present Study (RTL)	LOG	45 km	128	1.52*	1.51	1.04	2.08	0.22	0.019	1.3
Present Study (NL)	LOG	35–55 km	153	2.06*	1.97	0.96	5.6	0.68	0.055	2.7

* The difference in AM values for RTL and NL is statistically significant.

versus 15 ms). More than 80% of strokes that create new terminations on ground have leader durations longer than 8 ms, and more than 95% of strokes that follow the same channel have leader durations shorter than 8 ms. The exclusion of NL strokes likely creating new channel terminations was done in 20 out of 46 flashes and led to the reduction of the original sample of 211 NL strokes to 184.

Histograms of peak currents, directly measured at the rocket launcher for RTL strokes and estimated by the NLDN for NL strokes (median absolute current estimation error is about 15%; Mallick et al. (2014) [8].), are shown in Figs. 2a and b, respectively. The geometric mean (GM) values are 12.2 kA for RTL strokes and 14.5 kA for NL strokes. The difference is 19% or 16%, depending on which value is used as reference. The maximum value for RTL strokes is 38.4 kA vs. 54.5 kA for NL strokes. The corresponding histograms of preceding interstroke intervals (measured between return-stroke peaks in electric field records) are shown in Figs. 2c and d. Sample size in Fig. 2c ($N = 113$) is smaller than that in Fig. 2a ($N = 139$) because there is no interstroke interval prior to the initial stroke in RTL (in RTL, the first stroke, necessarily occurring in NL, is in effect replaced by the initial stage processes).

Although up to 15 kA the histograms for RTL and NL strokes are quite similar, the fraction of larger peak current events in the NL sample is larger. It is known (Schoene et al., 2010) [9] that the peak current is correlated with the return-stroke charge transfer, so that the contribution from the electrostatic field component can be larger for higher peak current strokes. Also, higher peak current strokes tend to have higher current rates of rise, which can influence the contribution from the radiation field component.

The interstroke interval can be viewed as a measure of channel decay prior to the RS, unless that interval contains a continuing current, which we did not consider in the present study. The amount of channel decay can potentially influence some RS current and, hence, electric field waveform parameters. It follows from Figs. 2c and d that the ranges of variation of interstroke intervals for RTL and NL strokes are generally similar. The GM for NL strokes is 63 ms, which very similar to its typical value (60 ms; Rakov and Uman, 2003, Chapter 4), and it is somewhat

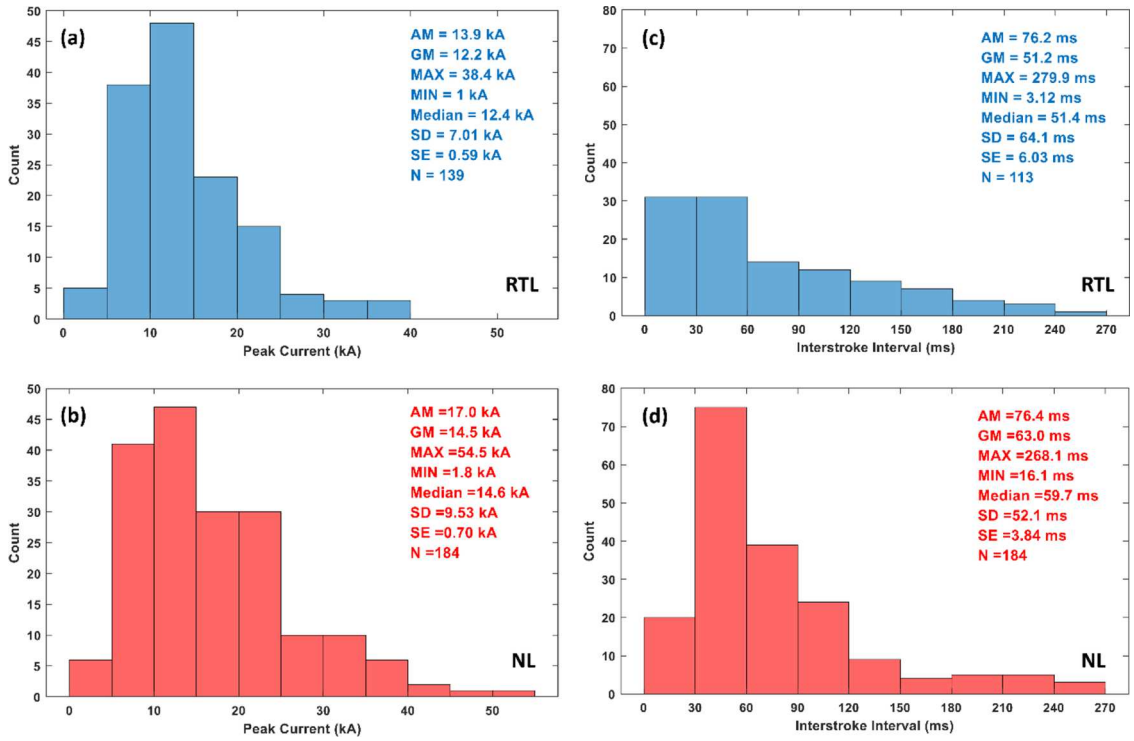

Fig. 2. Histograms of peak currents for (a) RTL strokes (directly measured) and (b) NL strokes (reported by NLDN) and of interstroke intervals for (c) RTL strokes and (d) NL strokes. (For interpretation of the references to colour in this figure legend, the reader is referred to the web version of this article.)

smaller (51.2 ms) for RTL strokes.

Parameters of return-stroke electric field waveforms, all recorded at LOG, that were examined in this study are: (A) 10-to-90% Risetime (t_{10-90}), (B) Half-Peak Width (t_{HPW}), (C) Initial Half-Cycle Duration (or Zero-Crossing Time (t_{ZC})), (D) Opposite-Polarity Overshoot Duration (t_{OS}), (E) Ratio of Electric Field Peak to Opposite-Polarity Overshoot (E_p/E_{OS}), (F) Fast-Transition 10-to-90% Risetime ($t_{FT10-90}$), (G) Slow-Front Duration (t_{SF}), (H) Slow-Front Magnitude Relative to Peak (E_{SF}/E_p). The definitions of these parameters are shown in Fig. 3 and are similar to those used in Haddad et al. [2012] [10] and Nag et al. [2012] [5].

4. Data presentation and results

In the following subsections, we present a total of eight parameters of electric field waveforms, for both RTL and NL strokes: 10-to-90% Risetime, Half-Peak Width, Initial Half-Cycle Duration (Zero-Crossing Time), Opposite Polarity Overshoot Duration, Ratio of Electric Field Peak to Opposite-Polarity Overshoot, Fast-Transition 10-to-90% Risetime, Slow-Front Duration, and Slow-Front Magnitude Relative to Peak. For each of these parameters, histograms and the following statistics are presented: arithmetic mean (AM), median, geometric mean (GM), maximum value (Max), minimum value (Min), standard deviation (SD), and standard error (SE) in the AM value, along with the sample size (N). For each parameter, we included a table showing comparison of the parameters for RTL and NL strokes based on data obtained in this study. Additionally included in the tables (just for completeness) are the parameters found in the literature. Detailed comparison with other studies is not done here, because our main objective was to eliminate possible influences of field propagation path and instrumentation on the results. Note that such comparison was previously done by Mallick and Rakov (2014) [6].

Standard error (SE) in the AM is defined as $SD/\sqrt{N}$ and can be used in evaluating the statistical significance of the difference between the AMs in different groups of events. It is often assumed that the difference is statistically significant if the intervals $(AM_i - 2SE_i)$ and $(AM_j + 2SE_j)$, where $AM_i > AM_j$, do not overlap. Note that the $(AM \pm 2SE)$ interval accounts for approximately 95% of the random variation of AM (e.g., McClave and Dietrich, 1979, p. 230 [11]). Sometimes SE is expressed in percent of AM as SE·100%/AM.

4.1. 10-to-90% risetime

Fig. 4a presents the histograms of 10-to-90% Risetime for RTL and NL strokes. Table 1 contains the detailed statistics and their counterparts found in the literature.

The AM and GM values of 10-to-90% Risetime for NL strokes are 2.5 μs and 2.2 μs, respectively, larger than 1.6 μs and 1.5 μs for RTL strokes. As per the procedure (criterion) described in the 2nd paragraph of Section 4, the difference in AM values is statistically significant.

4.2. Half-peak width

Fig. 4b presents the histograms of Half-Peak Width for RTL and NL strokes. Table 2 contains the detailed statistics and their counterparts found in the literature.

The AM and GM values of Half-Peak Width for NL strokes are 6.3 μs and 5.4 μs, respectively, which are larger than their counterparts, 3.8 μs and 3.1 μs, for RTL strokes. The difference in AM values is statistically significant. Similar to the 10-to-90% Risetime, the RTL data are characterized by less scatter than the NL data.

4.3. Initial half-cycle duration (zero-crossing time)

This parameter can be measured only in the waveforms that exhibit zero-crossing, as seen in Fig. 3a. We observed zero-crossing for 145 (79%) out of 184 NL strokes and 100 (72%) out of 139 RTL strokes. For comparison, Haddad et al. [2012] [10] found that for NL strokes in the 0–50 km range only 11% showed an opposite polarity overshoot and for those in the 50–100 km range 72% exhibited this feature. The lack of zero-crossing in far electric field waveforms is likely to be due to sizable

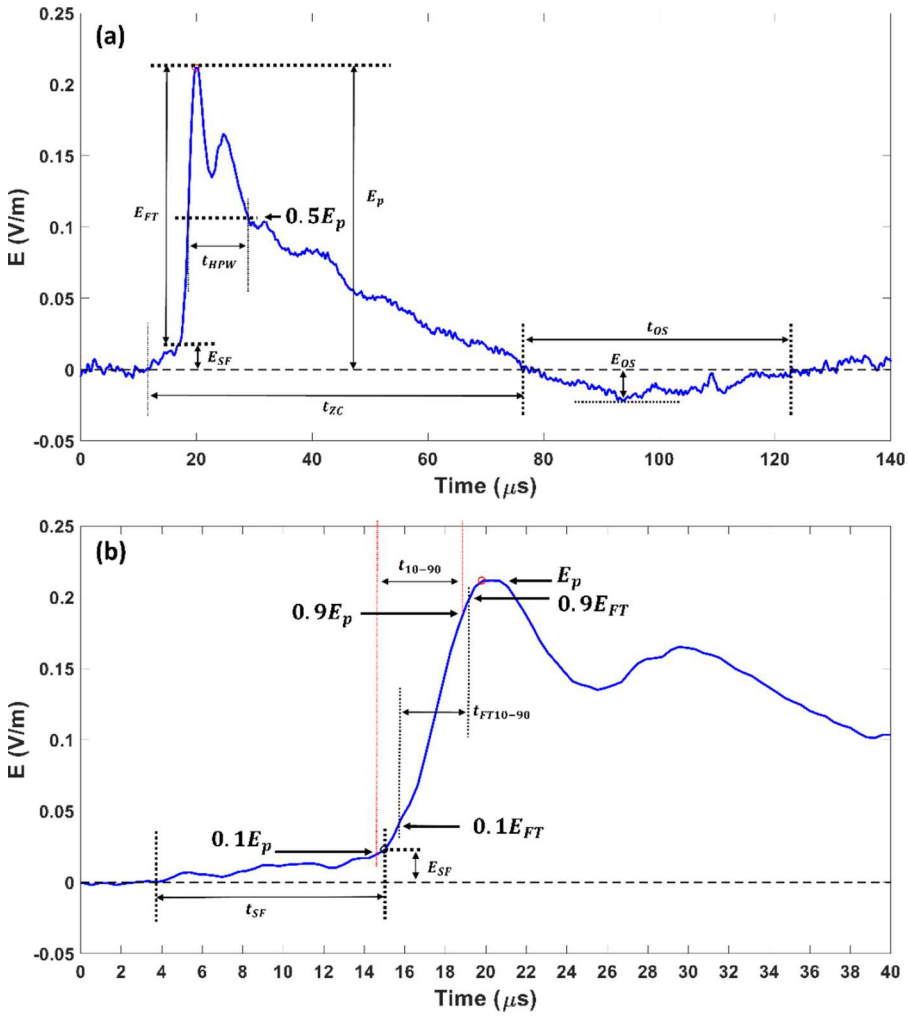

Fig. 3. Definitions of return-stroke electric field waveform parameters shown on (a) 140 μs and (b) 40 μs time scales, using a typical RTL stroke field waveform, with (b) being an expansion of (a). The waveform parameters include: 10-to-90% Risetime (t_{10-90}), Half-Peak Width (t_{HPW}), Zero-Crossing Time (t_{ZC}), Opposite-Polarity Overshoot Duration (t_{OS}), Ratio of Electric Field Peak to Opposite-Polarity Overshoot (E_p/E_{OS}), Slow-Front Duration (t_{SF}), Slow-Front Magnitude Relative to Peak (E_{SF}/E_p), and Fast-Transition 10-to-90% Risetime ($t_{ft10-90}$).

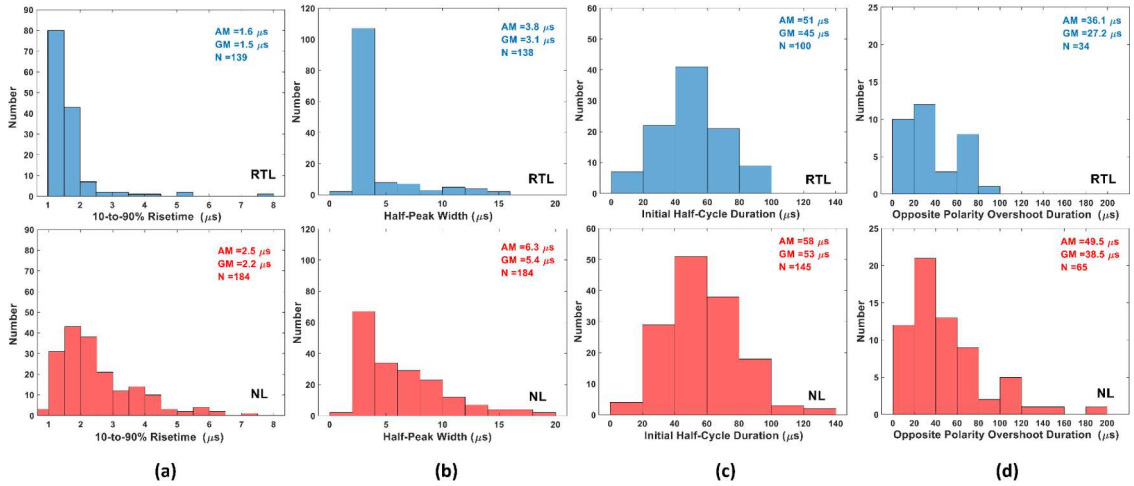

Fig. 4. Histograms of (a) 10-to-90% Risetime for RTL (top) and NL (bottom) strokes. (b) Half-Peak Width for RTL (top) and NL (bottom) strokes. (c) Initial Half-Cycle Duration for RTL (top) and NL (bottom) strokes. (d) Opposite Polarity Overshoot Duration for RTL (top) and RL (bottom) strokes.

contributions from the electrostatic and induction field components that overwhelm the expected Opposite Polarity Overshoot.

Fig. 4c presents the histograms of the Initial Half-Cycle Duration (zero-crossing time) and the detailed statistics are found in Table 3. The AM and GM values of Initial Half-Cycle Duration for NL strokes are 58 μs and 53 μs, respectively. The corresponding values for RTL strokes are 51 μs and 45 μs. The difference is not statistically significant, since the AM ± 2SE confidence intervals overlap.

4.4. Opposite polarity overshoot duration

Fig. 4d presents the histograms of Opposite-Polarity Overshoot Duration for RTL and NL strokes. Table 4 contains the detailed statistics and their counterparts found in the literature.

It is well known (e.g., Rakov and Uman, 2003, Chapter 4 [1]) that the far electric and magnetic field waveforms dominated by their radiation components are bipolar; that is, they exhibit zero-crossings and Opposite-Polarity Overshoots. These overshoots are reproduced by the engineering RS models that include current decay with height (for example, MTLL and MTLE models (e.g., Rakov and Uman, 2003, Chapter 12 [1])). The original transmission-line (TL) model, in which current magnitude and waveshape do not change with height, does not reproduce the opposite polarity overshoot, unless the current is turned off abruptly at the top of the channel, in which case the so-called mirror--image overshoot is produced (see, for example, Kato et al., 2021, Figs. 2 and 5 [15]). An additional reason for the Opposite-Polarity Overshoot occurrence is a change of lightning channel geometry from predominantly vertical to predominantly horizontal, as the upward propagating RS stroke enters the cloud (e.g., Cooray et al. 2008 [16]), which happens typically 25–75 μs after the RS onset. Recall that the typical Initial Half-Cycle Durations (zero-crossing times) are inside this range (see Figs. 4c).

The AM and GM values of the Opposite-Polarity Overshoot Duration are 49.5 μs and 38.5 μs, respectively, for NL strokes and 36.1 μs and 27.2 μs, respectively, for RTL strokes. Similar to the Initial Half-Cycle Duration, the difference in AM values is statistically not significant, since the AM ± 2SE confidence intervals overlap.

4.5. Ratio of electric field peak to opposite polarity overshoot

Histograms of the Ratio of Electric Field Peak to Opposite-Polarity Overshoot (labeled E_p and E_{os} in Fig. 3a) for RTL and NL strokes are shown in Fig. 5a, respectively. Table 5 contains the statistics from this study, as well as those found in the literature.

4.6. Slow-Front duration

Following Mallick and Rakov [2014] [6], in examining the Slow-Front Duration and Slow-Front Magnitude Relative to Peak, we distinguished between two types of slow front, which are labeled "classical type" (CT) and "plateau type" (PT). Slow fronts that exhibit an abrupt change followed by a relatively steady level are classified as "plateau type" (see Fig. 5f). All other (mostly concave) slow-front shapes are classified as "classical type" (see Fig. 3 and Fig. 5e). Percentages of PT Slow Fronts for RTL and NL strokes are 45% and 27%, respectively.

The histograms are shown in Fig. 5c and the statistics are given in Table 6. The differences in AM values for RTL and NL strokes in this study are not statistically significant.

As described in Section 3, we filtered out NL strokes that might have created a new termination on ground. There were a total of 27 such strokes, of which 22 exhibited discernible slow front (both CT and PT were observed). The AM SF duration for 22 NL strokes that likely created new terminations is 7.73 μs, which is considerably larger than AM = 4.85 μs for 153 NL strokes that likely followed the same channel, as expected. It is important to note that the latter comparison concerns only subsequent (as opposed to first) strokes.

4.7. Slow-front magnitude relative to peak

Fig. 5d presents the histograms of Slow-Front Magnitude Relative to Peak for RTL and NL strokes. Different shading is used for SFs of classical and plateau types. Table 7 contains the detailed statistics for each SF type individually and for both types combined, along with the results found in the literature.

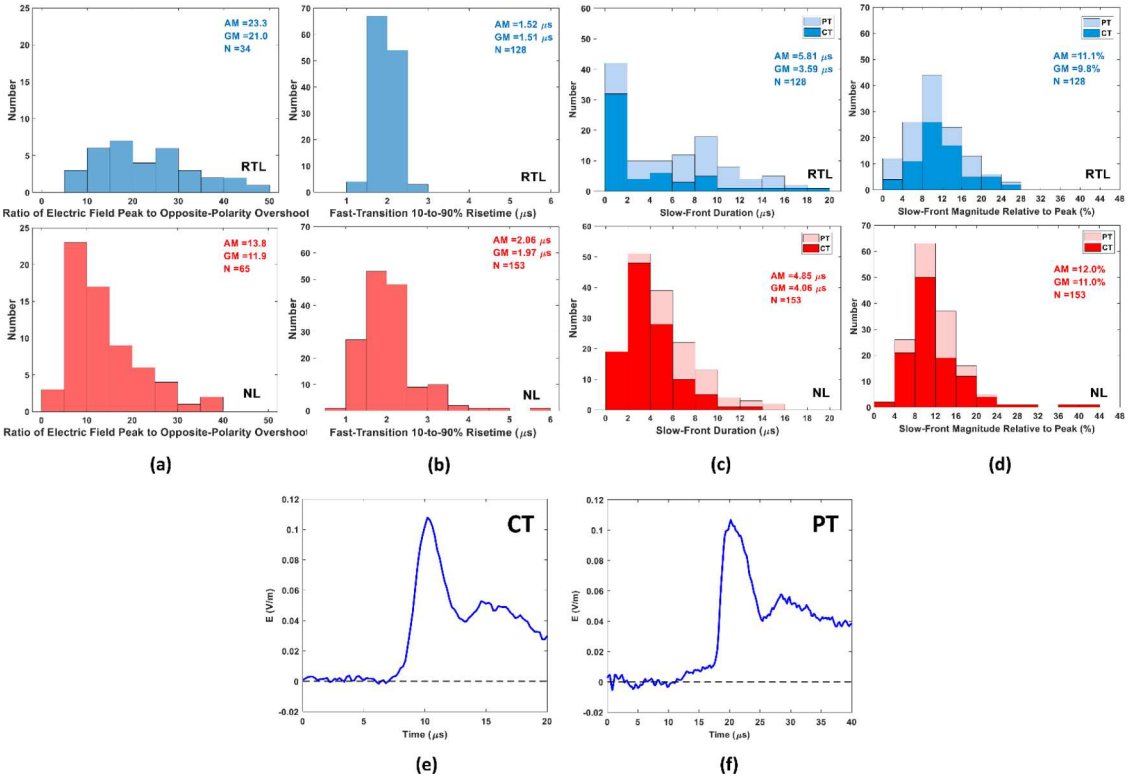

Fig. 5. (a) Histograms of (a) Ratio of Electric Field Peak to Opposite-Polarity Overshoot for RTL (top) and RL (bottom) strokes. (b) Fast-Transition 10-to-90% Risetime for RTL (top) and NL (bottom) strokes. (c) Slow-Front Duration for RTL (top) and NL (bottom) strokes. (d) Slow-Front Magnitude Relative to Peak for RTL (top) and NL (bottom) strokes. In (c) and (d), statistics are given for both CT and PT slow fronts combined. (e) and (f) are examples of CT and PT slow fronts, respectively.

This parameter for RTL strokes (AM = 11.1%) appears to be very similar to its counterpart for NL strokes (AM = 12%). The difference in AM values is not statistically significant for either CT or PT, or for both types combined.

4.8. Fast-Transition 10-to-90% risetime. Fig. 5d presents the histograms of Fast-Transition 10-to-90% Risetime for RTL and NL strokes. Table 8 contains the detailed statistics from this study and their counterparts found in the literature.

5. Discussion and summary

Le Vine et al. [1989] [2] measured electric field waveforms produced by 28 return strokes in rocket-triggered lightning (RTL) flashes at a distance of 5.16 km from the Kennedy Space Center (KSC) lightning triggering site, so that the initial portion of the field waveform was essentially radiation. They also measured electric field waveforms for 16 subsequent strokes in natural lightning (NL) at distances ranging from 29 to 39 km. In both cases the field propagation path was essentially entirely over water (brackish water for RTL and salt water for NL). Although the distances for NL were considerably larger than for RTL, it is reasonable to assume that in both cases the field waveforms were not significantly influenced by propagation effects. Le Vine et al. [1989] [2] compared the RTL and NL electric field waveforms (during the initial several microseconds) and summarized their findings as follows: "To a first approximation, the waveforms are very similar; however, the electric field changes from the triggered flashes tend to rise to peak faster and decay faster than do their counterparts in natural cloud-to-ground flashes". Specifically, the half-peak widths (HPWs) we measured in their average electric field waveforms for RTL and NL are 2 and 3.5 μs, respectively; that is, the HPW for NL return strokes is a factor of 1.75 larger than for their RTL counterparts. Le Vine et al. [1989] [2] could not measure zero-crossing times in their RTL field waveforms (because it does not occur at 5.16 km), nor did they examine this parameter in NL waveforms.

When fields propagate over land, the HPW values for subsequent strokes in NL are typically of the order of 10 μs. For example, we measured 10 μs in the waveform recorded at 65 km and reported by Haddad et al. [2012] [10] and 7 μs in the waveform recorded at 54 km and reported by Rakov [2013] [17]. In the present study, we found the AM and GM values of HPW for NL strokes at distances of 35–55 km to be 6.3 and 5.4 μs, respectively, vs. 3.8 and 3.1 μs for RTL strokes at 45 km, with the difference in AM values being statistically significant. Note that our ratios of the AM and GM values for NL and RTL (1.66 and 1.74, respectively) are very close to that (1.75) estimated from fields that propagated over water by Le Vine et al. [1989] [2].

We found that the E-field Initial Half-Cycle Duration (Zero-Crossing Time) for RTL is slightly smaller than for NL (51 μs vs. 58 μs in terms of AM and 45 μs vs. 53 μs in terms of GM). It is known (e.g., Zhu et al. [2018] [18]) that the field zero-crossing time reduces due (among other things) to a faster return-stroke current decay with height. In the modified transmission line model with exponential current decay with height (MTLE model), the current decay height constant λ is usually set to 2 km (Nucci et al. [1988] [19]). However, there are optical observations for RTL that are indicative of a stronger rate of current decay with height (smaller λ in the case of exponential current decay). Specifically, Wang et al. [1999] [20] reported that the luminosity peak for a return stroke in RTL decreased by about 30% within the lowest tens of meters of lightning channel. Also, for two triggered-lightning strokes, very strong current attenuation was inferred from luminosity measurements by Carvalho et al. [2015] [21]: to 47% and 38% of the peak current at the channel base at a height of 115 m, which corresponds to λ equal to 155 and 120 m, respectively. For natural-lightning return strokes, the luminosity peak (and by inference current peak) decay rate is considerably lower. For example, Jordan and Uman [1983] [22] found for seven subsequent return strokes in natural lightning an exponential decrease in the luminosity peak with height with a decay constant of 600 to 800 m. Thus, one of the reasons of smaller zero-crossing times for RTL compared to NL (although the difference in our study is not statistically significant) could be a faster current decay with height in RTL strokes. The same explanation probably applies to the smaller HPW for RTL strokes compared to NL strokes.

Saito and Ishii (2016) [23] presented modeling results suggesting that the far-field HPW can be significantly influenced by channel geometry (changing from vertical to more horizontal at an altitude of 200 m above ground level). The influence of horizontal channel section at the top of the vertical channel on the width of far-field waveforms was also examined by Cooray et al. (2008) [16], Ishii and Saito (2010) [25], Nag and Rakov (2015) [26], and Araki et al. (2018) [27] among others. Note that RTL channels in Florida are typically more or less vertical up to an altitude of about 5 km where they become more or less horizontal (Hill et al., 2013 [24]). Similarly, NL channels for subsequent strokes tend to become horizontal at altitudes of some kilometers (see, for example, Fig. 4.61 in Rakov and Uman (2003)). Therefore, we assume that, on average, the channel geometry of RTL strokes was not much different from that of subsequent strokes in NL.

In the present study, the AM and GM values of 10-to-90% Risetime for NL strokes are 2.5 μs and 2.2 μs, respectively, larger than 1.6 μs and 1.5 μs for RTL strokes. The difference in AM values is statistically significant. Note also that the 10-to-90% Risetime for RTL is less dispersed than for NL. The disparities could be related to the fact that the bottom of the channel in the case of RTL strokes is significantly influenced by the triggering-wire vapor/residue, while more diverse and less favorable conditions are probably encountered by NL strokes. Note that risetimes of the order of a few μs correspond to the RS travel distances of the order of a few hundred meters, which is similar to the triggering-wire length. For RTL strokes, Schoene et al. (2009) [28] found that the 10-to-90% current risetime depends on the electrical properties of the strike object (impedance seen by lightning at the strike point). This dependence is likely to translate into the far (radiation) electric fields, which would explain the larger variability of field risetimes for NL strokes.

Similar to the overall 10-to-90% Risetime, the Fast-Transition (FT) 10-to-90% Risetime for RTL strokes tends to be shorter and less dispersed than for NL strokes. The difference in AM values is statistically significant.

The AM and GM values of the Ratio of Electric Field Peak to Opposite-Polarity Overshoot for NL strokes are 13.8 and 11.9, smaller than their counterparts of 23.3 and 21 for RTL strokes. The difference in AM values is statistically significant. The shapes of the histograms for RTL and NL strokes are very different. If we assume that the histograms of electric field peaks for RTL and NL strokes are more or less the same, the difference would imply that Opposite-Polarity Overshoots for RTL strokes are less pronounced and more variable (maybe even affected by the accuracy of measurement of Opposite-Polarity Overshoot, when it is only a few percent of E_p).

We observed two types of slow front (SF), "classical type" (CT) and "plateau type" (PT), in both RTL and NL strokes. The PT occurs in RTL strokes more often than in NL strokes (45% vs. 27%). The SF duration represents the duration of the breakthrough phase (BTP) of the lightning attachment process (Rakov and Tran, 2019, [29]). BTP starts when the common streamer zone (CSZ) is formed and ends when the hot-channel connection is established, the latter being signified by the onset of FT in the field waveform. It is likely that the difference between the CT and PT SFs is related to the dynamics of the transformation of CSZ to a hot-channel link. For both the CT and PT slow fronts combined, the AM values for NL and RTL are 4.85 μs and 5.81 μs, respectively. The difference in AM values is not statistically significant, since the AM ± 2SE confidence intervals overlap. Similarly, for either CT or PT slow fronts taken separately, the difference in AM values is not statistically significant.

We examined correlation between the initial electric field peak (E_p)

and the various time parameters of field waveforms (see Fig. 3) and found it to be very low (determination coefficient $R^2 < 0.25$) to essentially none. In all cases, R^2 for NL strokes is considerably smaller than for RTL strokes.

In summary, far electric field waveforms for RTL strokes tend to be narrower and rise to peak faster than those for NL strokes. The corresponding statistical distributions for RTL strokes are less dispersed than for NL strokes. The differences in AM values are statistically significant and their reasonable explanations exist. Opposite-polarity overshoots for RTL strokes are less pronounced than for NL strokes. Plateau-type (as opposed to classical-type) slow fronts occur more often in RTL strokes than in NL strokes. The reason for this is presently not clear. The magnitudes of SF relative to peak for RTL and NL strokes are similar. Distributions of SF durations for RTL and NL strokes look different, but their average values are similar. Further research (both observations and modeling) is needed to better understand the reasons for the observed dissimilarities between the E-field waveforms produced by RTL and NL strokes, which is important because RTL strokes are often assumed to be representative of NL strokes.

CRediT authorship contribution statement

Z. Ding: Conceptualization, Data curation, Formal analysis, Investigation, Methodology, Software, Validation, Visualization, Writing – original draft, Writing – review & editing. **S. Chen:** Data curation, Software, Writing – review & editing. **V.A. Rakov:** Conceptualization, Formal analysis, Investigation, Project administration, Funding acquisition. **Y. Zhu:** Conceptualization, Data curation, Formal analysis, Methodology, Validation. **I. Kereszy:** Writing – review & editing. **M.A. Uman:** Supervision, Writing – review & editing.

Declaration of Competing Interest

The authors declare that they have no known competing financial interests or personal relationships that could have appeared to influence the work reported in this paper.

Data Availability

All the data used in this study can be found at: https://doi.org/10.6084/m9.figshare.20100722.v1.

Acknowledgements

This research was supported in part by NSF Grant AGS-2055178. The authors would like to thank William Brooks of Vaisala Inc. for providing NLDN data. Triggered-lightning experiments at Camp Blanding would not be possible without efforts of many individuals, including, in alphabetical order, W. R. Gamerota, J. D. Hill, D. M. Jordan, T. Ngin, and J. T. Pilkey, to name some of them who deserve special thanks. Also, the authors thank A. Nag, D. Tsalikis, S. Mallick, R. Olsen, and M. Tran for their significant contributions to setting up and/or operating the LOG instrumentation. Three anonymous reviewers provided useful comments on the paper.

References

[1] V.A. Rakov, M.A. Uman, Lightning: Physics and Effects, Cambridge (2003).
[2] D.M. Le Vine, J.C. Willett, J.C. Bailey, Comparison of fast electric field changes from subsequent return strokes of natural and triggered lightning, J. Geophys. Res. (1989).
[3] R.J. Fisher, G.H. Schnetzer, R. Thottappillil, V.A. Rakov, M.A. Uman, J. D. Goldberg, Parameters of triggered-lightning flashes in Florida and Alabama, J. Geophys. Res. (1993).
[4] C.D. Weidman and E.P. Krider, "The fine structure of lightning return stroke waveforms," vol. 83, no. 8, 1978.
[5] A. Nag, et al., Characteristics of the initial rising portion of near and far lightning return stroke electric field waveforms, Atmos. Res. 117 (Nov. 2012) 71–77.
[6] S. Mallick, V.A. Rakov, Characterization of far electric field waveforms produced by rocket-triggered lightning, in: 2014 Int. Conf. Light. Prot. ICLP, 2014, pp. 1527–1534, 2014.
[7] V.A. Rakov, S. Mallick, A. Nag, V.B. Somu, Lightning Observatory in Gainesville (LOG), Florida: a review of recent results, Electr. Power Syst. Res. 113 (2014) 95–103.
[8] S. Mallick, et al., Performance characteristics of the NLDN for return strokes and pulses superimposed on steady currents, based on rocket-triggered lightning data acquired in Florida in 2004-2012, J. Geophys. Res. Atmos. 119 (7) (Apr. 2014) 3825–3856.
[9] J. Schoene, M.A. Uman, V.A. Rakov, Return stroke peak current versus charge transfer in rocket-triggered lightning, J. Geophys. Res. Atmos. 115 (12) (2010) 1–7.
[10] M.A. Haddad, V.A. Rakov, S.A. Cummer, New measurements of lightning electric fields in Florida: waveform characteristics, interaction with the ionosphere, and peak current estimates, J. Geophys. Res. Atmos. (2012).
[11] F.H. McClave, J.T. Dietrich, Statistics, Dellen Publishing Company, San Francisco, CA, 1979.
[12] M. Master, M. Uman, W. Beasley, M. Darveniza, Lightning induced voltages on power lines: experiment, IEEE Trans. Power Appar. Syst. PAS-103 (9) (Sep. 1984) 2519–2529.
[13] Y.T. Lin, et al., Characterization of lightning return stroke electric and magnetic fields from simultaneous two-station measurements, J. Geophys. Res. 84 (C10) (1979) 6307.
[14] V. Cooray, S. Lundquist, Characteristics of the radiation fields from lightning in Sri Lanka in the tropics, J. Geophys. Res. 90 (D4) (1985) 6099–6109.
[15] N. Kato, J. Yamamoto, Y. Baba, T.H. Tran, V.A. Rakov, FDTD simulations of LEMP propagation in the earth-ionosphere waveguide using different lightning models, IEEE Trans. Electromagn. Compat. 63 (4) (2021) 1107–1117.
[16] V. Cooray, V.A. Rakov, F. Rachidi, R. Montaño, C.A. Nucci, On the relationship between the signature of close electric field and the equivalent corona current in lightning return stroke models, IEEE Trans. Electromagn. Compat. 50 (4) (2008) 921–927.
[17] V.A. Rakov, Electromagnetic methods of lightning detection, Surv. Geophys. 34 (6) (2013) 731–753.
[18] Y. Zhu, V.A. Rakov, M.D. Tran, W. Lyu, D.D. Micu, A modeling study of narrow electric field signatures produced by lightning strikes to tall towers, J. Geophys. Res. Atmos. 123 (18) (2018) 10, 260-10277.
[19] C.A. Nucci, C. Mazzetti, F. Rachidi, and M. Lanoz, "On lightning return stroke models for LEMP calculations," in *19th International Conference on Lightning Protection,* Graz, *April*1988.
[20] D. Wang, N. Takagi, T. Watanabe, V.A. Rakov, M.A. Uman, Observed leader and return-stroke propagation characteristics in the bottom 400m of a rocket-triggered lightning channel, J. Geophys. Res. Atmos. 104 (D12) (1999) 14369–14376.
[21] F.L. Carvalho, M.A. Uman, D.M. Jordan, T. Ngin, Lightning current and luminosity at and above channel bottom for return strokes and M-components, J. Geophys. Res. Atmos. 120 (20) (Oct. 2015) 238.
[22] D.M. Jordan, M.A. Uman, Variation in light intensity with height and time from subsequent lightning return strokes, J. Geophys. Res. 88 (C11) (1983) 6555–6562.
[23] M. Saito, M. Ishii, Attenuation effect of lossy ground on peak electromagnetic intensities investigated by method of moments, in: 24th International Lightning Detection Conference, 2016.
[24] J.D. Hill, et al., Correlated lightning mapping array and radar observations of the initial stages of three sequentially triggered Florida lightning discharges, J. Geophys. Res. Atmos. 118 (15) (2013) 8460–8481.
[25] M. Ishii, M. Saito, Influence of geometry of lightning channel on associated electromagnetic field waveforms, Prz. Elektrotechniczny 86 (8) (2010) 1–5.
[26] A. Nag, V.A. Rakov, A transmission-line-type model for lightning return strokes with branches, Electr. Power Syst. Res. 118 (2015) 3–7.
[27] S. Araki, Y. Nasu, Y. Baba, V.A. Rakov, M. Saito, T. Miki, 3-D finite difference time domain simulation of lightning strikes to the 634-m Tokyo skytree, Geophys. Res. Lett. 45 (17) (2018) 9267–9274.
[28] J. Schoene, et al., Characterization of return-stroke currents in rocket-triggered lightning, J. Geophys. Res. Atmos. 114 (3) (2009) 1–9.
[29] V.A. Rakov, M.D. Tran, The breakthrough phase of lightning attachment process: from collision of opposite-polarity streamers to hot-channel connection, Electr. Power Syst. Res. 173 (October 2018) 122–134, 2019.
[30] J. Wang, Q. Li, Li Cai, Mi Zhou, Y. Fan, J. Xiao, A. Sunjerga, Multiple-Station Measurements of a Return-Stroke Electric Field From Rocket-Triggered Lightning at Distances of 68–126 km, IEEE TRANSACTIONS ON ELECTROMAGNETIC COMPATIBILITY 61 (2) (2019) 440–448, https://doi.org/10.1109/TEMC.2018.2821193.